J. Mod. Transport. (2017) 25(3):194–204
DOI 10.1007/s40534-017-0136-8

www.springer.com/40534

Comparative analysis of cast-in-place post-tensioned and steel–concrete composite bridge bent caps

Nur Yazdani[1] · **Francisco D. B. Ruiz**[2]

Received: 31 March 2017 / Revised: 27 June 2017 / Accepted: 29 June 2017 / Published online: 21 July 2017

Abstract The complexity of the IH-635 Managed Lanes Project, located in Dallas County, Texas, posed several technical and constructive challenges, leading to the adoption of solutions different from the traditional. Two alternative solutions for the pier cap on one of the bridge crossings over IH-35E in the IH-635 project were analyzed in this case study, a cast-in-place post-tensioned concrete cap and an innovative prefabricated steel–concrete composite cap. The approach was to use an estimation of direct costs for material and labor and consideration of construction time schedules. A supplementary numerical modeling confirmed that both alternatives behave elastically under imposed loads. The direct cost of material and labor for the two alternatives were close. However, the composite alternative required 13 days less construction time, resulting in substantial cost savings from traffic closing in the very busy traffic corridor. Traffic closing costs were substantially higher than the direct costs, especially for the post-tensioned cap. The quantification of the benefits allows more confidence in the utilization of the composites caps, leading to faster completion of bridge projects and substantial economic savings.

Keywords Bridge pier cap · Bridge bent · Post-tensioned structure · Steel–concrete cap · Cost estimation · Construction schedule · Traffic closing cost

1 Introduction

Structural concrete prefabricated systems have been successfully used with the well-known advantages of construction time reduction and the number of operations to be performed in situ, improved quality control, work zone safety improvement and lower environmental impact. Unlu [1] proposed various precast concrete systems for the construction of abutments and bent caps. Billington et al. [2] proposed concrete precast systems for the construction of single- and double-column inverted T hammerhead pier caps with connection details. Matsumoto et al. [3] developed a precast concrete system for pile bent caps for non-seismic regions with several connection details. Other systems have been applied successfully. For example, precast post-tensioned supported bent caps with an inverted T-section with spans up to 17.68 m were used for the U-section bridges in the project mentioned herein. However, there is a practical limit for the span lengths due to the self-weight that can impact safe lifting and placement.

The evolution of pier cap design is a consequence of the intensive use of bridges caused by the changes in the transportation infrastructures [4]. In general, abutment design has been extensively analyzed [4], particularly for integral abutments. Barr et al. [5] investigated the spalling of an integral abutment bridge in Salt Lake City, UT, through monitoring and finite element modeling. Nikravan [6] studied the behavior of integral bridges subjected to temperature variations using 3D finite element models. However, pier choices are generally limited to CIP

✉ Nur Yazdani
Yazdani@uta.edu

Francisco D. B. Ruiz
rudy270183@gmail.com

[1] Department of Civil Engineering, University of Texas at Arlington, Arlington, TX 76019, USA

[2] Structural Engineer, Ferrovial-Agroman, Dallas, TX 75211, USA

concrete supported either by one hammerhead bent cap or more than one column and pile bent cap [7]. Some special types (straddle bent caps) are briefly addressed elsewhere [8]. Public agencies have guidelines on the design of the most common bent cap types, such as rectangular column bent caps [9, 10], inverted T column bent caps [9, 10] and hammerhead bent caps [11]. However, comparative design/construction guidance for alternates is lacking.

Nicholas et al. [12] compared the reinforcing requirements of the strength design approach for flexure and shear and the strut-and-tie model method in their application to hammerhead pier design. Pereira [13] analyzed the behavior of hammerhead piers reinforced with T-headed bars and different levels of prestressing in the cantilever ends by static load testing. Kerley [14] developed finite element models to analyze the behavior of the connections between reinforced concrete bent caps and cast-in-shell piles under lateral loads. Bracci et al. [15] experimentally studied unexpected cracks in the cantilevered regions of concrete bent caps under service loads. The flexural cracking was related to the stress levels in longitudinal reinforcement below the service stress limits. Billington [16] experimentally studied the structural behavior of two-span continuous bent caps with different levels of prestress. Several past studies involved integral piers. For example, Ales [17] developed a connection detail between an integral steel cap girder and concrete piers, while Wassef et al. [18] developed specifications and design examples for integral steel box-beam pier caps. Denio et al. [19] studied the shear strength and reinforcing details for connections between steel bent caps and concrete piers through static load testing.

It is apparent that a comparative study of the two alternative bent caps considered herein has not been undertaken in the past. The cast-in-place post-tensioned cap is a more traditional approach, while the steel–concrete composite cap is a more innovative solution. Possible cost and time savings from the composite cap utilization, if demonstrated, would allow the possible consideration and adoption of this type and other types of innovative bent cap solutions.

2 Case study background

The IH-635 managed lane construction project is located in North Dallas, Texas, and involves both IH-35E and IH-635 freeways (Fig. 1). Started in early 2011, it was completed and opened to traffic in summer of 2015. It has dramatically increased the traffic capacity of this important Dallas corridor, consisting of four to six general purpose lanes, two managed lanes and two to three frontage roads in each direction. A new loop 12–IH-635 westbound direct connector was built, needing the construction of a new bridge

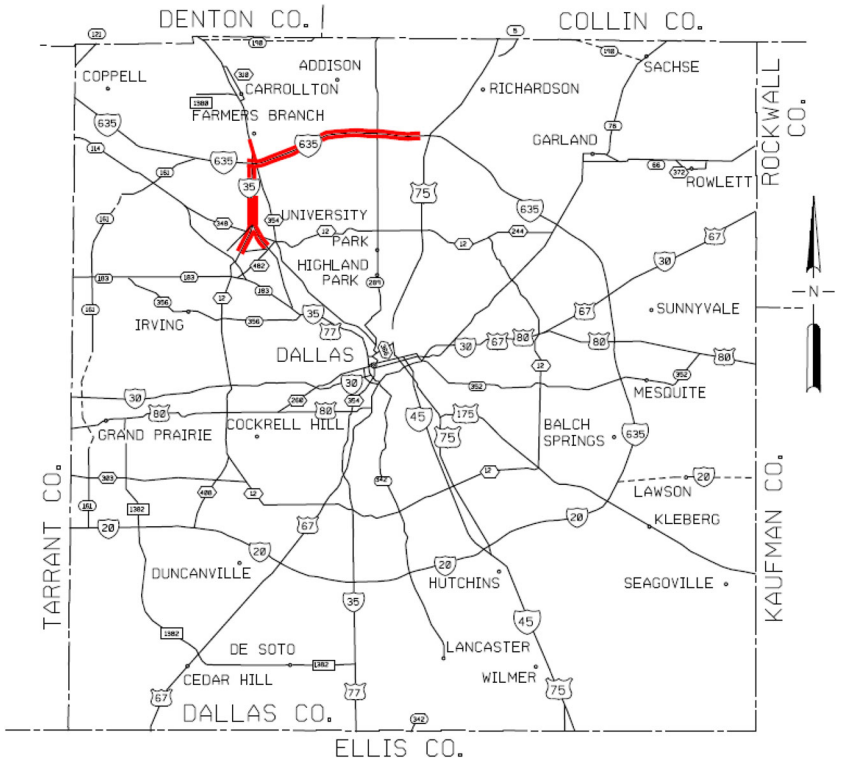

Fig. 1 Project location

(Bridge 4) to crossover IH-35E northbound, as seen in Fig. 2. This is a major traffic corridor, supporting high traffic volume, particularly during rush hours. The construction of a new bridge using conventional design and construction techniques on this corridor could result in significant lane closings, impacting traffic and overall economic activity.

Fig. 2 Bridge 4 crossing over IH-35E, in service

The originally conceived and designed post-tensioned cast-in-place (CIP) concrete bent cap could not be built without a lengthy closure of IH-35E for the required formwork and concrete curing times. As a result, the design team considered as alternate an innovative prefabricated bent cap solution simply supported on columns and straddling the highway underneath that could limit the traffic impact. With bent spans varying from 22.7 to 26.2 m (Fig. 3), the two alternative precast designs considered were: (1) a precast prestressed concrete bent cap and (2) a composite steel–concrete bent cap, consisting of a rectangular-shaped steel section with a top CIP concrete slab. The two alternatives reduced the various constructability issues associated with the original CIP concept that would include time-consuming post-tensioning of tendons at an elevated position. The second alternative involves simply lifting and placing the steel–concrete section once the concrete slab reached enough strength to support its self-weight.

Bridge 4 (Fig. 3) is the focus of this paper. With a total length of 304.8 m, the bridge consists of nine spans with three Tx54 standard concrete girders [20, 21] per span, with

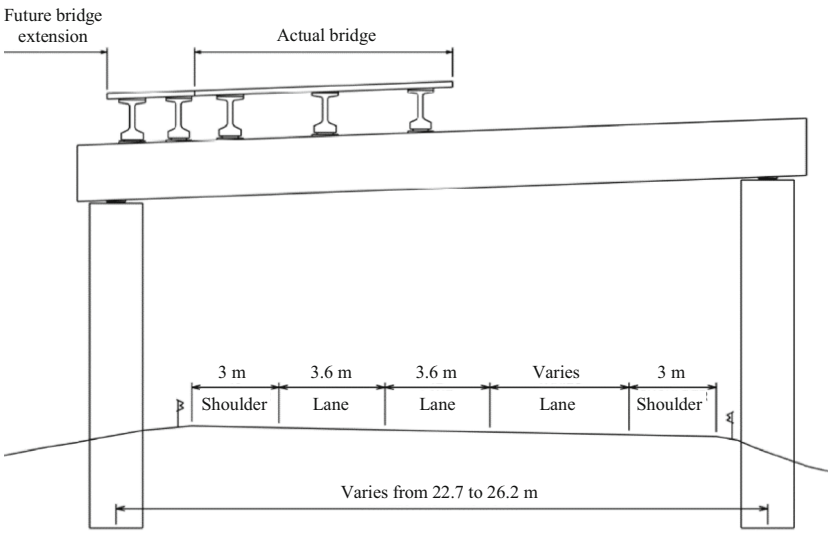

Fig. 3 Bridge 4 typical section

Table 1 Details of alternatives

Alternatives	Section	Reinforcement	Concrete compressive strength	Diaphragms	Steel section strength
Post-tensioned concrete	1.93 m wide, 2.59 m deep	6 Parabolic tendons, 31–15 mm dia. grade 270 low lax type	41.4 MPa; 34.5 MPa at jacking	N/A	N/A
Composite steel–concrete	1.83 m wide, 1.73 m deep, with 250 mm concrete slab at top		41.4 MPa	Two at each support and additional girder stiffeners	Grade 50

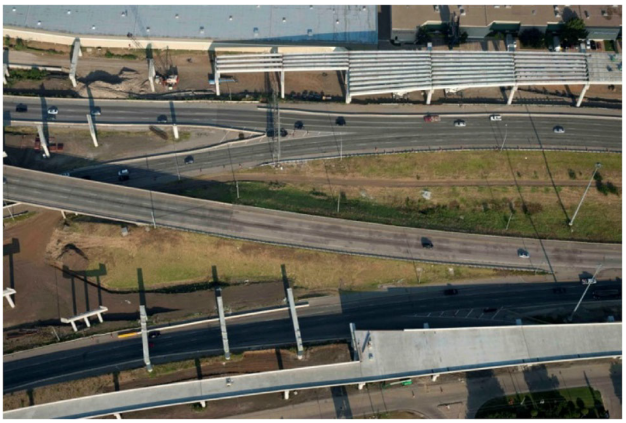

Fig. 4 Bridge 4 construction, bent caps 7, 8 and 9 in place

Fig. 5 Bridge 4 construction, girders in place

the exception of span three that has three steel plate girders. The future lateral extension of the bridge with two new girders per span was considered in the design. Spans 6–9 and bent caps 7–9 were built over the IH-35E roadway. The two precast alternatives discussed previously for bent 7 (22.7 m span length) in Bridge 4 were analyzed herein for structural behavior, cost and construction schedule. The characteristics of the two alternatives are presented in Table 1. They were considered as simply supported on two CIP 1.83-m-diameter concrete columns. Elastomeric bearing pads and a shear key were employed to ensure the end conditions. Bent 7 carries the loads from spans 6 and 7 (Figs. 4, 5).

The current bridge construction market conditions, with increasing competitiveness among the construction companies, have made the design optimization key for large transportation projects. Therefore, a theoretical comparative study between the two alternatives in terms of structural behavior, cost-efficiency and construction time was undertaken and presented in this paper [22].

3 Finite element modeling (FEM)

The FEM software ABAQUS [23] includes several material models that were considered herein. For concrete in both alternatives, the concrete damage plasticity (CDP) model was used in this study, intended for brittle materials with the possibility of establishing failure criteria by damage parameters. Both tension and compression are treated as linear elastic–plastic, and tension stiffening is used to model the tension post-failure behavior and reinforcement interaction. This is the most realistic concrete model in ABAQUS. The concrete was modeled using a 3D deformable tetrahedral homogeneous solid element, due to its ability to better adapt to any member geometry. Although mesh refinement needed is usually smaller if quadratic elements are used, only linear elements were utilized in this study because they are more accurate for plastic behavior. For concrete, AASHTO provides a Poisson's ratio of 0.2 [24]. The CDP default parameters were taken herein as follows: dilatation angle 36°, eccentricity 0.1 and viscosity parameter 0 [25]. In the absence of experimental data, the approach suggested by Wight and MacGregor [26] for the concrete compressive behavior was used herein, valid for concrete strengths from 13.8 to 124 MPa. The needed damage parameters were adopted

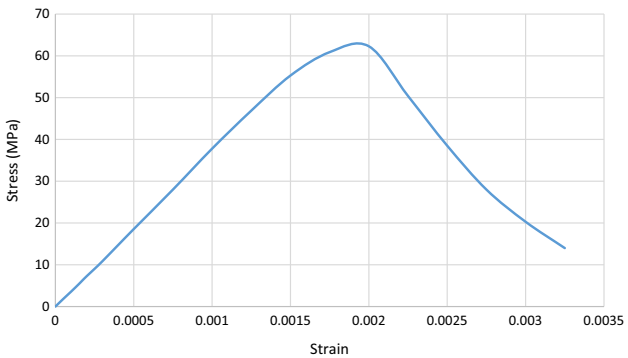

Fig. 6 Concrete compression stress–strain curve

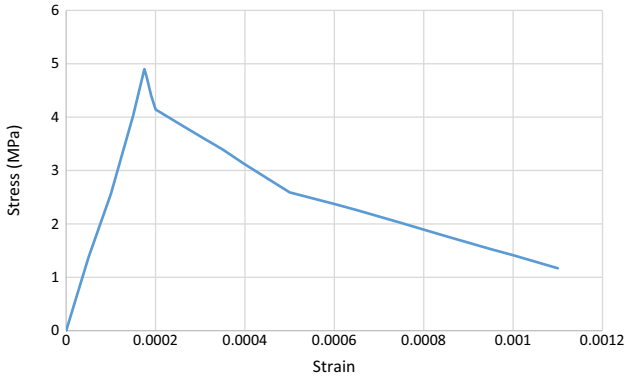

Fig. 7 Concrete tension stress–strain curve

Table 2 Girder reactions on bent cap

Girder line	Total reaction (kN)
1	1,270
2	1,489
3	1,927
4	2,362
5	2,474

from Birtel and Mark [27]. A maximum stress and the corresponding strain must be defined as a limit for total compression crushing failure of the concrete and were taken as 0.5 and 0.3 times the concrete compressive strength, respectively [28]. The resulting concrete compressive stress–strain model is presented in Fig. 6.

A simplified tensile concrete stress–strain relationship, as shown in Fig. 7 [28], was used herein with an elastic behavior up to the modulus of rupture. The subsequent discharge branch that defines the plastic behavior of the material is approximated with three line segments.

The regular steel rebars in concrete for both alternatives were modeled as 3D wire elements with truss sections (capable of developing only axial stresses) with a cross-sectional area equal to the rebar area. To guarantee the deformation compatibility and proper stress transmission between concrete and rebar, the reinforcement was embedded into the concrete section (host region). By doing so, the degrees of freedom of the truss elements were constrained by the adjacent concrete solid elements. The Grade 60 reinforcing steel was modeled with an elastic–perfectly plastic behavior and a yield strength of 413.7 MPa. A steel modulus of elasticity of 200,000 MPa with a Poisson's ratio of 0.3 was assumed.

The prestressing steel for the post-tensioned alternative 1 was also modeled as elastic–plastic, with the following properties: modulus of elasticity of 196,500 MPa, Poisson's ratio of 0.3, ultimate strength of 1,861 MPa, yield strength of 1,675 MPa, ultimate tensile strain of 0.035, 31 strands of 15 mm diameter each and nominal area of 4,340 mm^2 per tendon.

For alternative 2, the structural steel stress–strain curve was also assumed to be elastic–perfectly plastic. The A709 Grade 50 steel had a modulus of elasticity of 200 GPa, Poisson's ratio of 0.3 and yield strength of 345 MPa. The steel section was modeled using 3D deformable shell elements. The top flange was tied to the bottom surface of the concrete slab to guarantee deformation compatibility. Using the tie interaction, the nodal degrees of freedom in the slab surface were constrained by those on the cap surface. Three types of stiffeners were included: diaphragms at support locations, girder stiffeners at girder locations and interior stiffeners distributed along the length of the member. They were modeled with 3D deformable homogeneous shells. Proper interaction between the cap section and the stiffeners was achieved through merging.

The two alternate models were subjected to AASHTO HL-93 loading [24]. The loads applied to the bent caps consisted of the following: (1) girder reactions at supports for the controlling load combination (strength I) obtained by considering the superstructure self-weight (girder, deck, curbs and barriers), the lane load and the truck or tandem load; and (2) factored bent cap self-weight for the critical load combination (strength I). The cap concrete and the structural steel unit weights were assumed as 23 and 77.8 kN/m^3, respectively. The girder reactions were determined with the software PGSuper [20, 21] by modeling the two bridge spans that load the pier cap. This is a windows-based software for the design, analysis and load rating of multi-span precast–prestressed bridge girders in accordance with the AASHTO LRFD specifications. Table 2 summarizes the girder reactions on the bent cap. Cap models supported 10 girders (five from the backward span and five from the forward span).

Simple support conditions on the piers were assumed for the bent caps and were achieved through the release of support constraints as needed. Releasing the rotation at supports minimized the moment transferred to the columns.

Figure 8 shows the prestressing tendon profile view of the alternate 1 bent cap. The effect of the post-tensioning tendons was modeled as a combination of homogeneous axial compressive stress and a vertical force from the draped tendons, from the load-balancing method. Because the contribution of prestressing steel to the stiffness of the section is minimum [29], actual prestressing tendons were not included in the FEM. The compressive force applied at the ends was determined by deducting the prestress losses from the jacking force. The load-balancing force was obtained by imposing equilibrium at the tensioned tendon.

The prestress force at jacking per tendon was 4,328 kN. The effective prestress was obtained using AASHTO LRFD procedure [24]. The total loss of prestress was

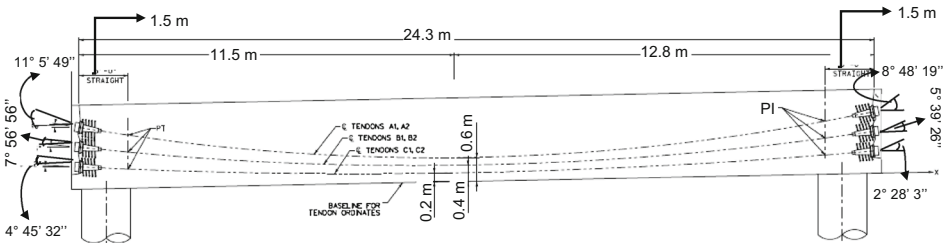

Fig. 8 Post-tensioned cap details and tendon profiles

Table 3 Mesh sizes

Alternatives	Mesh sizes tried (mm)	Maximum no. of nodes
1. Post-tensioned	381–127	77,000
2. Composite	381–76	83,000

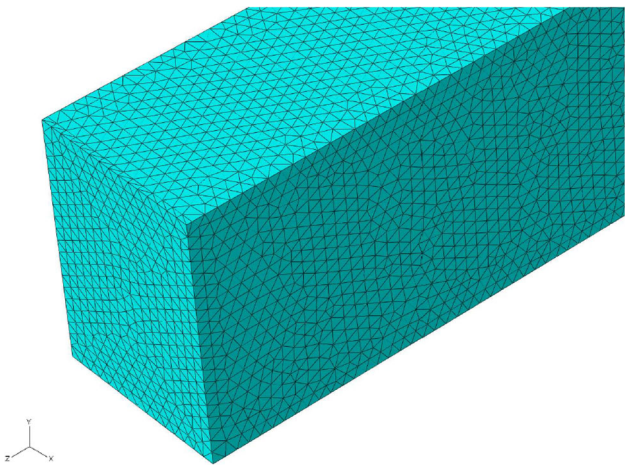

Fig. 9 Post-tensioned cap model with 127 mm mesh size

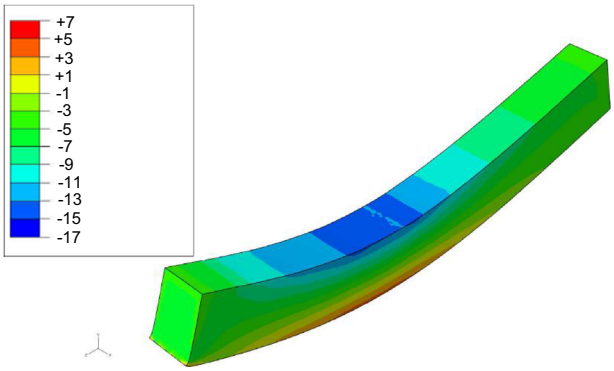

Fig. 10 Post-tensioned cap model, bending stress distribution

determined as the sum of the short-term losses (elastic shortening of 20 MPa, friction loss of 54 MPa, anchorage set loss of 76 MPa) and long-term losses (shrinkage/creep, steel relaxation) of 249 MPa, resulting in a total loss of 399 MPa. The approximate method given by AASHTO LRFD, article 5.9.5.3, was used herein to find the long-term losses, with an assumed relative humidity of 70%. The resulting effective prestress was 1,144 MPa. A total prestress loss of 399 MPa was obtained, resulting in the net long-term prestress force of 4,328 kN per tendon.

Table 3 shows the mesh details used herein. Figure 9 shows the alternate 1 model with 127 mm mesh size. Computer run times were found to be exceedingly high for mesh sizes below the minimum mesh size shown.

Simplified elastic hand calculations performed herein were used to validate the FEM. The contribution of the longitudinal steel to the section strength was neglected. The solution obtained implied close match between the FEM and the hand-calculated stresses. The concrete elements remained within the elastic limits for both top and bottom fiber stresses. As can be seen, the FEM adequately simulated the structural behavior of the bent cap (Fig. 10).

The plan and section views for the alternative 2 composite cap are shown in Figs. 11 and 12, respectively. Figure 13 shows the composite cap meshed view with 76 mm mesh size, and Fig. 14 shows the bending stresses distribution in the steel section part.

4 Cost estimate and schedule

Accurately determining the cost of a construction project is a difficult task that needs experience, engineering judgment and scientific principles [30]. Different methods are available for the estimator depending on the project stage and information available, and accuracy needed [31]. The direct cost of the pier cap alternatives considered herein was estimated for comparison purposes.

The following materials would be needed for the construction of the post-tensioned bent cap: concrete with a 28-day compressive strength of 41.4 MPa; grade 60 reinforcing steel; grade 270 low relaxation prestressing steel; and other materials, such as grout, plastic ducts and end anchorages. The construction process would consist of the following activities: (1) shoring structure placement until

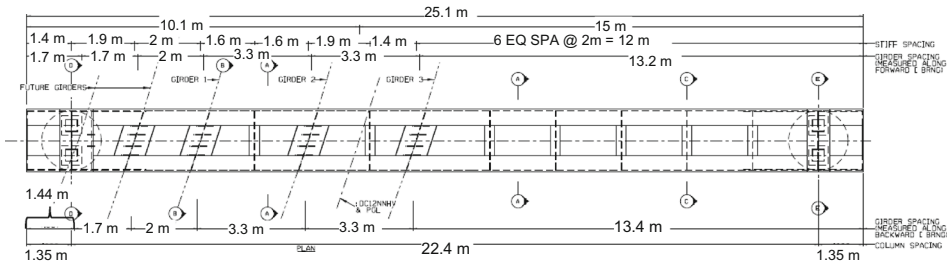

Fig. 11 Plan view geometry of steel–concrete composite cap

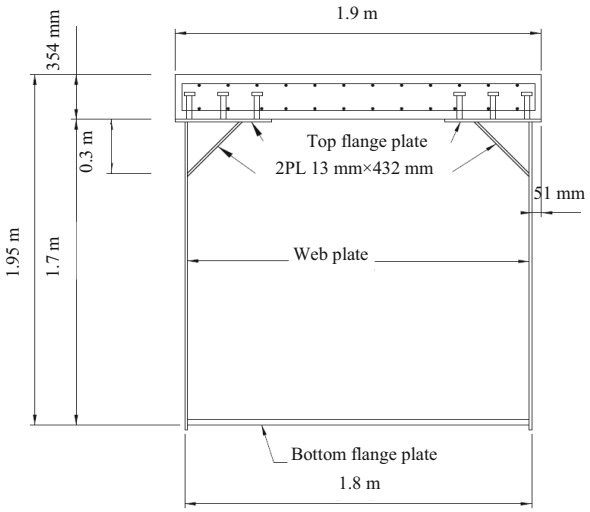

Fig. 12 Composite cap typical section

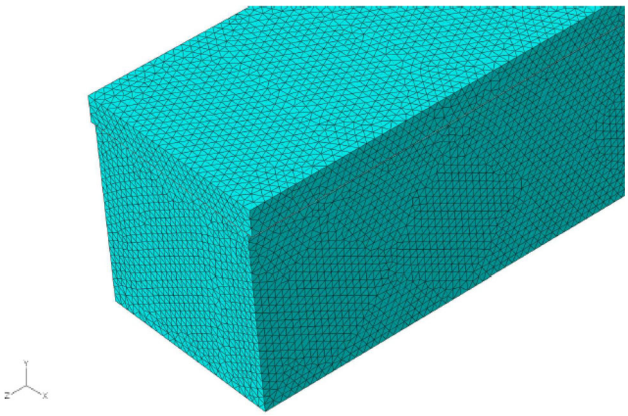

Fig. 13 Composite cap model, 76-mm mesh detail

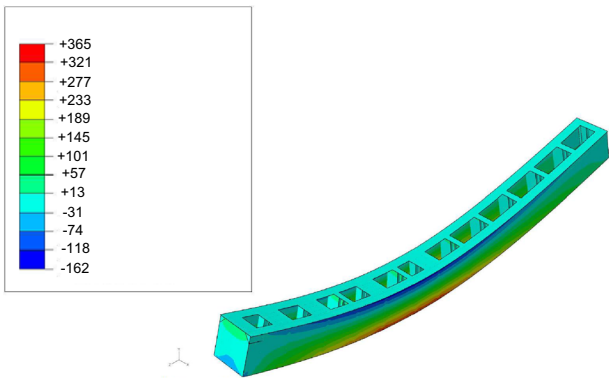

Fig. 14 Bending stresses distribution in steel section, alternative 2 (MPa)

the cap reaches sufficient strength; (2) long-term closure of traffic in the roadway below the cap until the end of the cap construction process; (3) form work; (4) rebar cage fabrication and placement performed simultaneously with previous activities; (5) placement of additional elements for prestressing tendons (ducts and end anchorages), simultaneously with the previous tasks; (6) concrete casting with sufficient curing time to achieve the minimum required strength to perform the next two activities; (7) tendon placement, stressing and duct grouting; and (8) form work and shoring structure removal.

For typical moist-cured concrete with type I cement, the variation of strength with time is defined in Eq. 1 [26]:

$$f'_{ci} = \frac{t}{4.00 + 0.85t} f'_c, \tag{1}$$

where f'_{ci} denotes concrete strength at time t; t curing time (days); and f'_c nominal 28-day concrete strength.

Considering the 28-day concrete compressive strength of 41.4 MPa and a required strength at post-tension jacking of 34.5 MPa, a minimum duration of 12 days after concrete casting would be needed before the tendons could be stressed.

The following materials would be needed for the construction of the composite bent cap: concrete with a nominal compressive strength of 41.4 MPa, Grade 60 reinforcing steel and A709 Grade 50 structural steel. The construction process would require a lower number of activities than the post-tensioned cap process, as follows: (1) concrete slab form work. The steel section is placed on ground and the slab formwork is placed on it, also at

Fig. 15 Lifting of composite bent cap

ground level; (2) slab rebar placement also at ground level; (3) slab concrete casting also at ground level. Enough curing time has to be provided prior to removing the form work. (4) Slab form work removal; and (5) lifting and placement of the composite cap in place on already built CIP columns (Fig. 15).

Considering a minimum required concrete strength of 20.7 MPa for lifting, from Eq. 1, the lifting and placement of the composite cap could not take place before 4 days after slab casting. IH-35E highway would have to be closed to traffic during Task 5. Because of the short time required to place the cap on its final position, only one night closure of IH-35E would be needed.

The cost of a project development can be obtained as the summation of the following costs for each of the materials and activities: First is direct cost of material, labor and equipment. This cost, provided that the construction process is optimized, should not significantly vary with the construction company performing the work. And second is indirect cost of traffic closure and detour.

Two sets of values were needed to estimate the direct cost: (1) unit cost for each of the identified materials and activities. The unit costs used in this study were actual average costs. (2) Quantity takeoff for each of the materials and activities. For cost estimation purposes, the previously described activities were grouped in some cases. The direct cost consequence of the closure of IH-35E southbound freeway for both cap options (lane closure cost) and the associated indirect cost of impacted economic activity were also considered herein.

For the indirect cost of traffic closure and detour, the following analysis is based on partly site-specific and partly general information. The southbound lanes of IH-35E freeway carry an average daily traffic of 113,676 [32] vehicles of which 8% are single-unit trucks and 4% are combination trucks. A 1.6-km work zone with a 24 h/day four lane closures is assumed herein in effect between Walnut Hill Lane and Royal Lane until the construction is complete. The travel delay cost is a summation of the following costs:

1. Delay cost for passenger vehicles. This cost was based on the estimated unit value of personal travel time for passenger cars [33–36] and unit value of business travel time [33]. The weighted average of travel time values for passenger cars considering both personal and business travel were then computed, and the delay costs for passenger cars on the northbound lanes estimated as $535,478/day.
2. Delay cost for trucks. This cost was estimated based on the unit value of truck travel time [34, 35, 37, 38]. The delay costs for both single-unit and combination trucks on the northbound lanes were then projected as $92,675/day [37, 38].
3. Time-related vehicle depreciation cost. The hourly time-related depreciation costs for vehicle types were estimated herein [37, 38]. The time-related depreciation cost for passenger cars, single-unit and combination trucks on the northbound lanes were then projected as $51,884/day [34, 35].
4. Freight inventory delay cost. The hourly cost of freight inventory values was obtained from literature [39]. Then, the number of loaded freight trucks were estimated [37, 38], and the associated cost of freight inventory delay calculated as $589/day [40].
5. Miscellaneous costs were estimated as $25,275/day for vehicle operating cost (VOC) and $14,664/day for crash cost [41]. VOCs are the expenses incurred by road users as a result of vehicle use. Crash costs are associated with work zones and related detours, and are a function of the expected change in the crash rates due to the presence of work zones [41].

Based on the above estimates, the grand total cost due to lane closures on I-35E southbound freeway at the construction site was found as approximately $720,567/day. Gantt charts showing the time schedule of construction are presented in Figs. 16 and 17. The total calculated direct costs were $207,281 and $202,735 for the post-tensioned cap and the composite cap, respectively, as shown in Tables 4 and 5, similar for the two alternatives. However, the lane closure cost of closing IH-35E makes the cast-in-place option much less economic. It may be noted that the construction of the post-tensioned cap would require 23 days, of which traffic would be impacted on 12 days. However, the composite cap would need only 10 days of construction time, of which only one day (actually, a few hours during a night) would have traffic impact. Therefore, the composite alternative had a significant advantage in terms of construction and traffic disruption times. This is

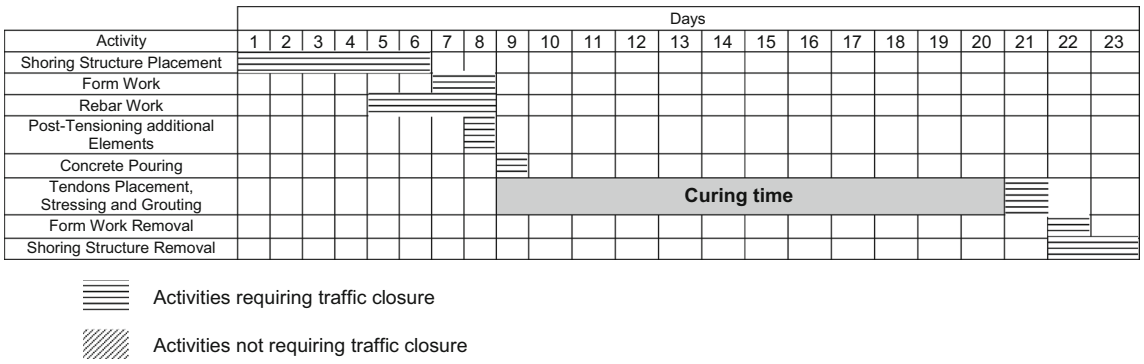

Fig. 16 Post-tensioned bent cap construction schedule

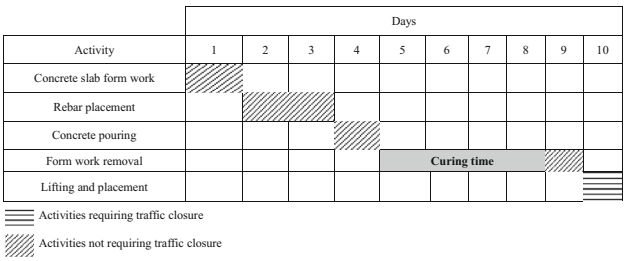

Fig. 17 Composite bent cap construction schedule

apparent in the total traffic disruption costs for the two alternatives, a very high $8.6 million for the post-tensioned cap, but only $720 k for the composite cap. It is apparent that the traffic disruption cost is the major savings aspect for the latter option. The post-tensioned cap option is overall 23 times more expensive than the composite cap option.

Above features an analysis performed for the city of Dallas, Texas, in one of the most heavily populated highways in the metroplex, using a Federal Highway Administration program [41]. The costs associated with lane closures are multi-faceted, and some are difficult to quantify. The main cost factors associated with the traffic impact were included herein. Factors such as noise and its impact on business and local communities are hard to estimate. Another associated factor is emission cost of vehicles. There is no current consensus on how to assign a dollar value to quantify the impacts of each emission pollutant type. Lifetime maintenance cost for the two alternatives were not included herein. Because of the need to periodically restore the corrosion protective coating on the steel cap section, the composite cap would have a higher maintenance cost overall than the post-tensioned cap.

The expected duration of the construction activities was obtained by surveying construction engineers who worked on the cap project. Because of the importance of minimizing traffic disruptions on the major freeways, it was assumed that the work would be performed during all seven days of the week. To estimate the time of IH-35E traffic impact during construction, activities that would impact the traffic were differentiated from those that would not.

The one disadvantage of the proposed composite bent cap is the additional flexibility with large deflections. This requires the fabrication of the steel section with a predefined camber to comply with the serviceability limits.

If different cap types are used for the two pier caps supporting a span, the difference in the deflection

Table 4 Post-tensioned cap cost estimate

Item	Description	Total quantity	Unit cost ($)	Total cost ($)
Direct costs				
Concrete (material)	Only material	126 m^3	113	14,238
Concrete (placement)	Includes form work and shoring tower placement and removal, and concrete pouring	126 m^3	1,054	132,804
Reinforcing steel	Includes material and labor	13,956 kg	1.04	14,514
Prestressing steel	Tendon, including all additional elements, grout and tendon tensioning	155 m	295	45,725
		Total direct costs	$207,281	
Indirect costs				
Lane closure		12 days	720,567	8,646,804
		Grand total cost	8,854,085	

Table 5 Composite cap cost estimate

Item	Description	Total quantity	Unit cost ($)	Total cost ($)
Direct costs				
Concrete (material)	Only material	12.5 m^3	113	1,413
Concrete (placement)	Includes form work and shoring tower placement and removal, and concrete pouring	12.5 m^3	743	9,287
Reinforcing steel	Includes material and labor	10,901 kg	1.04	13,417
Grade 50 steel	Steel in finished steel cap section including lifting	21,264 kg	8.40	178,618
		Total direct costs		$202,735
Indirect costs				
Lane closure		1 day	720,567	720,567
		Grand total cost	923,302	

developed at each end can generate additional stresses in the superstructure and slab joints. This effect can be amplified for cases like span 7 considered herein, where one of the exterior girders is located near the point of maximum deflection in the cap (Fig. 3).

From the evaluation of the direct costs, construction schedule and traffic impacts, the composite cap was considered a far superior alternative overall.

5 Conclusions

1. Computer modeling and cost estimation can be effectively used to comparatively evaluate highway bridge bent cap options. Prefabricated steel section with cast-in-place composite concrete deck can be an innovative and economic substitute for the more typical cast-in-place post-tensioned concrete bridge bent cap, especially for wide bent cap spans.
2. Both bent cap types studied herein performed adequately under elastic behavior. The top and bottom stresses were within the material elastic ranges.
3. The total direct costs of material and construction for the post-tensioned and the composite bent caps were comparable.
4. The required construction time for the composite bent cap alternative is about half the construction time for the post-tensioned alternative. The associated traffic impact for the composite alternative is very short (only one night), as opposed to 12 days for the post-tensioned alternative. This is a big advantage, especially when the construction related lane closure would involve a major interstate highway in a congested metropolitan area.
5. The estimated I-35 E southbound lane closure and traffic impact cost was $720 k/day. Due to the extended traffic closure needs for the post-tensioned bent cap alternative, the total traffic closure cost was estimated as $8.6 million for this alternative, as opposed to only $720 k for the composite alternative. It is obvious that traffic impact costs are the primary cost drivers for the two alternatives, as compared to the material/labor costs. The roughly 23 times additional lane closure cost for the post-tensioned alternative makes it less economically attractive than the composite alternative.

Acknowledgements Ferrovial-Agroman, Inc. is gratefully acknowledged herein for allowing the use of various data from the LBJ Project in the development of this paper.

References

1. Unlu D (2010) Rapid bridge construction technology: precast elements for substructures. Thesis, University of Wisconsin-Madison
2. Billington S, Barnes R, Breen J (1998) A precast substructure design for standard bridge systems. In: Research Report 1410-2F for Texas Department of Transportation, Center for Transportation Research. The University of Texas at Austin
3. Matsumoto EE, Waggoner MC, Sumen G, Kreger ME, Wood SL, Been JE (2001) Development of a precast bent cap system. Center for Transportation Research. University of Texas at Austin. Research Report 1748-2
4. Zhao JZ, Tonias DE (2012) Bridge engineering: design, rehabilitation, and maintenance of modern highway bridges. McGraw-Hill, New York
5. Barr PJ, Halling MW, Huffaker C, Boyle H (2013) Behavior and analysis of an integral abutment bridge. Utah State University, Logan
6. Nikravan N (2013) Structural design issues for integral abutment bridges. Dissertation, Ryerson University

7. Chen WF, Duan L (2014) Bridge engineering handbook: substructure design. CRC Press, Boca Raton
8. Coletti D, Sheahan J (2012) Steel bridge design handbook: substructure design. Federal Highway Administration, Washington
9. TxDOT (Texas Department of Transportation) (2010) Inverted tee bent cap design example. In: Design example is in accordance with the AASHTO LRFD Bridge Design Specifications, as prescribed by TxDOT Bridge Design Manual - LRFD (May 2009). Bridge Division, Austin, TX
10. TxDOT (Texas Department of Transportation) (2010) Rectangular bent cap design example. In: Design example is in accordance with the AASHTO LRFD Bridge Design Specifications, as prescribed by TxDOT Bridge Design Manual - LRFD (May 2009). Bridge Division, Austin, TX
11. AZDOT (Arizona Department of Transportation) (2007) LRFD substructure example 3. Hammerhead pier on spread footing
12. Nicholas T, Barth KE, Boyajian DM (2011) A simplified approach to bridge substructure design. Geotech Geol Eng 29(1):27–35
13. Pereira RM (1994) Behavior of structural concrete cantilever piers using T-Headed reinforcing bars and varied prestressing design criteria. Thesis, The University of Texas at Austin
14. Kerley RF (2013) Finite element analysis of reinforced concrete pile caps to cast-in-shell Steel Piles. Thesis, Tennessee Technological University
15. Bracci JM, Keating PB, Hueste MB (2000) Cracking in RC bent caps. Texas Department of Transportation. Research Report 1851-1
16. Billington SL (1994) Behavior of two-span continuous pier caps with varying levels of prestress. Thesis, The University of Texas at Austin
17. Ales JM (1994) The connection between an integral steel cap girder and a concrete pier. Dissertation, University of Texas at Austin
18. Wassef WG, Davis D, Srithatan S, Werff JRV, Abendroth RE, Redmond J, Greimann L (2004) Integral steel box-beam pier caps. In: Transportation research board of the national academies. NCHRP REPORT 527
19. Denio RJ, Yura JA, Kreger ME (1995) Behavior of reinforced concrete pier caps under concentrated bearing loads. Texas Department of Transportation. University of Texas at Austin. Research Report 1302-1
20. TxDOT (Texas Department of Transportation) (2015) Bridge standards. Austin
21. TxDOT (Texas Department of Transportation) (2015) PGSuper resource center. Austin. http://www.pgsuper.com/content/txdot. Accessed on 26 June 2015
22. Ruiz FDB (2015) Comparative analysis of cast in place post-tensioned and steel-concrete composite bridge bent caps. M. S. Thesis, University of Texas at Arlington, Arlington, TX
23. Dassault Systems (2016) ABAQUS unified FEA. http://www.3ds.com/products-services/simulia/products/abaqus/. Accessed on 16 May 2015
24. AASHTO (American Association of State Highway and Transportation) (2012) AASHTO LRFD bridge design specifications
25. Kmiecik P, Kaminski M (2011) Modelling of reinforced concrete structures and composite structures with concrete strength degradation taken into consideration. Arch Civil Mech Eng 11(3):623–636
26. Wight JK, MacGregor JG (2012) Reinforced concrete. Mechanics and design. Pearson, New Jersey
27. Birtel V, Mark P (2006) Parameterised finite element modeling of RC beam shear failure. In: ABAQUS user's conference. Ruhr-University Bochum, Germany, pp 95–107
28. Wahalathantri BL, Thambiratnam DP, Chan TH, Fawzia S (2011) A material model for flexural crack simulation in reinforced concrete elements using ABAQUS. In: Proceedings of the 1st annual international conference on engineering, designing and developing the built environment for wellbeing. Queensland University of Technology, pp 260–264
29. Saiedi MR (2007) Load-deflection response of a prestressed concrete T-beam. Thesis, Queen's University, Ontario
30. Bhargava A (2009) A probabilistic evaluation of highway project costs. Purdue University, West Lafayette
31. Pratt D (2011) Fundamentals of construction estimating. DELMAR CENGAGE Learning, Alberta
32. NCTCOG (North Central Texas Council of Governments) (2016) Traffic count information system. NCTCOG. http://www.nctcog.org/trans/data/tcins/. Accessed on 23 Sept 2016
33. NHTS (National Household Travel Survey) (2009) NHTS online analysis tool. CTA, ORNL. http://nhts.ornl.gov/tools.shtml. Accessed on 24 Sept 2016
34. U.S. BLS (Bureau of Labor Statistics) (2010) Employment cost trends. Bureau of labor statistics. http://www.bls.gov/oes/tables.htm. Accessed on 24 Sept 2016
35. U.S. BLS (Bureau of Labor Statistics) (2010) Employment cost trends. Bureau of labor statistics. http://www.bls.gov/ncs/ebs/benefits/2010/. Accessed on 24 Sept 2016
36. US Census (2010) Income. Census. http://www.census.gov/topics/income-poverty/income.html. Accessed on 24 Sept 2016
37. FHWA (Federal Highway Administration) (2005) Highway economic requirements system-state version. In: Technical report, HERS-ST, Washington, DC
38. FHWA (Federal Highway Administration) (2005) HERS-ST technical manual. In: Highway economic requirements system-state version, technical report, Washington, DC
39. Alam M, Rajamanickam G (2007) Development of truck payload equivalent factor. Submitted to FHWA Office of Freight Management and Operations
40. U.S. BEA (Bureau of Economic Analysis) (2010) Implicit price deflators for gross domestic product. Bureau of Economic Analysis. http://www.bea.gov/iTable/iTable.cfm?. Accessed on 24 Sept 2016
41. FHWA (Federal Highway Administration) (2015) Work zone user costs: concepts and applications. US DOT. http://www.ops.fhwa.dot.gov/wz/resources/publications/fhwahop12005/index.htm. Accessed on 15 Sept 2016